

Article

Responses of Urban Wetland to Climate Change and Human Activities in Beijing: A Case Study of Hanshiqiao Wetland

Yong Zhang ¹, Bo Cao ^{1,2}, Qiyue Zhang ², Shifeng Cui ¹, Baoshan Cui ^{2,*} and Jizeng Du ^{2,*} 

¹ Beijing Shunyi Hanshiqiao Wetland Nature Reserve Management Center, Beijing 101309, China; catherinecai@mail.bnu.edu.cn (Y.Z.); cb@bnu.edu.cn (B.C.); 202021180062@mail.bnu.edu.cn (S.C.)

² State Key Joint Laboratory of Environmental Simulation and Pollution Control, School of Environment, Beijing Normal University, Beijing 100875, China; 201911180156@mail.bnu.edu.cn

* Correspondence: cuibs@bnu.edu.cn (B.C.); dujz@bnu.edu.cn (J.D.); Tel.: +86-010-5880-2079 (B.C.); +86-181-0125-1586 (J.D.); Fax: 010-58802079 (B.C.)

Abstract: Hydrological connectivity is an essential indicator of wetland pattern and functional stability. The reduction of connectivity usually means the degradation of wetland ecological function, internal energy flow, and nutrient cycle disturbance. Taking Hanshiqiao wetland as a case, we used Morphological Spatial Pattern Analysis (MSPA) with the Connectivity Index (IIC, Integral Index of Connectivity; PC, Probability of Connectivity) to analyze the change in hydrological connectivity of Hanshiqiao Wetland from both spatial and temporal aspects. The results showed that the hydrological connectivity of Hanshiqiao Wetland significantly improved with the implementation of the wetland restoration project. According to the changes in MSPA function types, the spatial morphological evolution of Hanshiqiao Wetland can be divided into two stages: the recovery stage and the stable stage. In the restoration stage, the area of the core wetland gradually increased, and many croplands and islet wetlands were transformed into the core wetland. The area of the core wetland recovered from 33 hm² in 2005 to 119 hm² in 2020. However, during the stable period, the landscape pattern of Hanshiqiao Wetland did not change significantly, and the hydrological connectivity of the wetland was mainly affected by water resource supply. In general, during the restoration period of Hanshiqiao Wetland, the changes in core wetlands played a leading role in the hydrological connectivity of Hanshiqiao Wetland. In the stable period, the main factors affecting the hydrological connectivity of Hanshiqiao Wetland are upstream recharge water, land-use change, and climate change. However, with climate warming and population surge, upstream water supply gradually decreases, and Hanshiqiao Wetland faces an increasingly severe water resource crisis. Therefore, to maintain the hydrological connectivity of Hanshiqiao Wetland, it is necessary to increase the artificial ecological water supply. The combined MSPA model and grey relational analysis method can better reveal the evolution characteristics and driving mechanism of wetland hydrological connectivity, which can provide a methodological reference for other wetland-related research.

Keywords: hydrological connectivity; Morphological Spatial Pattern Analysis (MSPA); urban wetland; grey relational analysis; spatial morphology



Citation: Zhang, Y.; Cao, B.; Zhang, Q.; Cui, S.; Cui, B.; Du, J. Responses of Urban Wetland to Climate Change and Human Activities in Beijing: A Case Study of Hanshiqiao Wetland. *Sustainability* **2022**, *14*, 4530. <https://doi.org/10.3390/su14084530>

Academic Editor: Miklas Scholz

Received: 11 February 2022

Accepted: 6 April 2022

Published: 11 April 2022

Publisher's Note: MDPI stays neutral with regard to jurisdictional claims in published maps and institutional affiliations.



Copyright: © 2022 by the authors. Licensee MDPI, Basel, Switzerland. This article is an open access article distributed under the terms and conditions of the Creative Commons Attribution (CC BY) license (<https://creativecommons.org/licenses/by/4.0/>).

1. Introduction

A wetland ecosystem is a functional unit with high ecological vulnerability in nature, and its hydrological connectivity is critical to maintaining the stability and comprehensive benefits of the whole ecosystem. Wetland ecosystem functions are realized by a series of interconnected hydrological processes such as collecting, storing, filtering, or discharging water; deposition; and dissolution [1]. From the perspective of ecohydrology, hydrological connectivity refers to the mutual transfer of matter, energy, and organic matter among various elements of a water cycle island through a water network [2]. Quantifying the hydrological connectivity of wetlands can help determine wetland conservation and restoration priorities and evaluate the best location for wetland drainage or restoration [3].

After many years of research, the study of hydrological connectivity has made significant progress in ecology [4–6]. However, the methods for studying and assessing hydrological connectivity are still elementary and cannot meet relevant research needs [7]. Existing studies are committed to exploring the hydrological connectivity of the wetland ecosystem to find the methods to optimize the restoration of wetland ecosystem services [8]. At present, the main methods for studying and assessing hydrological connectivity include the geostatistical connectivity method, infiltration theory, graph theory/network theory, the Connectivity Index, etc. [9–13]. These methods are still elementary and cannot meet relevant research needs. Connectivity indexes, such as IIC (Integral Index of Connectivity) and PC (Probability of Connectivity), closely link the ecological process threshold, patch properties, and other elements with the spatial information and have been widely used in research to achieve specific results [14–16]. However, these methods just provide a highly generalized index, which lacks information on spatial patterns [17].

Recently, MSPA (Morphological Spatial Pattern Analysis), a morphology-based pattern analysis method, has been successfully applied to analyze morphological changes of various landscapes, showing strong applicability [18–20]. MSPA is a mathematical model targeted at describing the geometry and connectivity of image components [21,22]. MSPA applies to any digital image based on the geometric concept at a different scale. However, existing MSPA-based analysis mainly focuses on constructing and optimizing forests, green infrastructure, and ecological network patterns [23–25]. This method is rarely applied in the study of wetland hydrological connectivity, and studies are limited to analyzing the fragmentation of wetland patches.

With rapid urbanization, the area of urban wetland has been degraded in China [26,27]. The wetlands not only lack water but have also been polluted significantly due to climate change and human overuse of water. The core wetland is gradually being fragmented into small patches, the wetland's ecological function has been depleted, and the urban wetland's biodiversity has been reduced considerably. This phenomenon is more evident in Beijing, Shanghai, and other supercities [28,29]. As a typical natural wetland in Beijing, Hanshiqiao Wetland has undergone significant changes due to the disturbance of climate change and human activities. Therefore, it is helpful to understand the evolution characteristics and driving factors of urban wetlands by studying the hydrological connectivity evolution characteristics of Hanshiqiao Wetland [30].

To quantify the changes in the hydrological connectivity of wetlands, we took six high-resolution remote sensing images of Hanshiqiao Wetland in 2005, 2007, 2009, 2011, 2014, and 2020 as data sources. Then, we combined the MSPA model with the IIC and PC indexes to quantify the overall and local structure-function of the wetland hydrological connectivity. Furthermore, we identify the evolution process of the spatial pattern for the hydrological connectivity from the restoration to the stable phase. Additionally, the factors of hydrological connectivity change drivers are discussed in this paper. The research results can provide a theory for the protection and restoration of wetlands with similar problems.

2. Dataset and Method

2.1. Study Area

Hanshiqiao Wetland Nature Reserve is located at Yangzhen and Lishui town, Shunyi District, northeast Beijing. It is about 35 km away from the center of Beijing. The total area of Hanshiqiao Wetland is 1900 ha (see Figure 1). The core area is the inundated area under the perennial water level of Hanshiqiao Reservoir and the marsh at the water edge, which is within 5–10 m outside the isolated ditch by the roadside lake, with 163.5 ha. Along the periphery of the core area, the average distance of 5–10 m is the buffer zone, with an area of 12.1 ha. Besides the core area, the protected area includes the experimental area and a buffer zone of 100 ha. Dense reed marshes and rich biodiversity form a unique ecological landscape in the Beijing suburb plain [28,31,32].

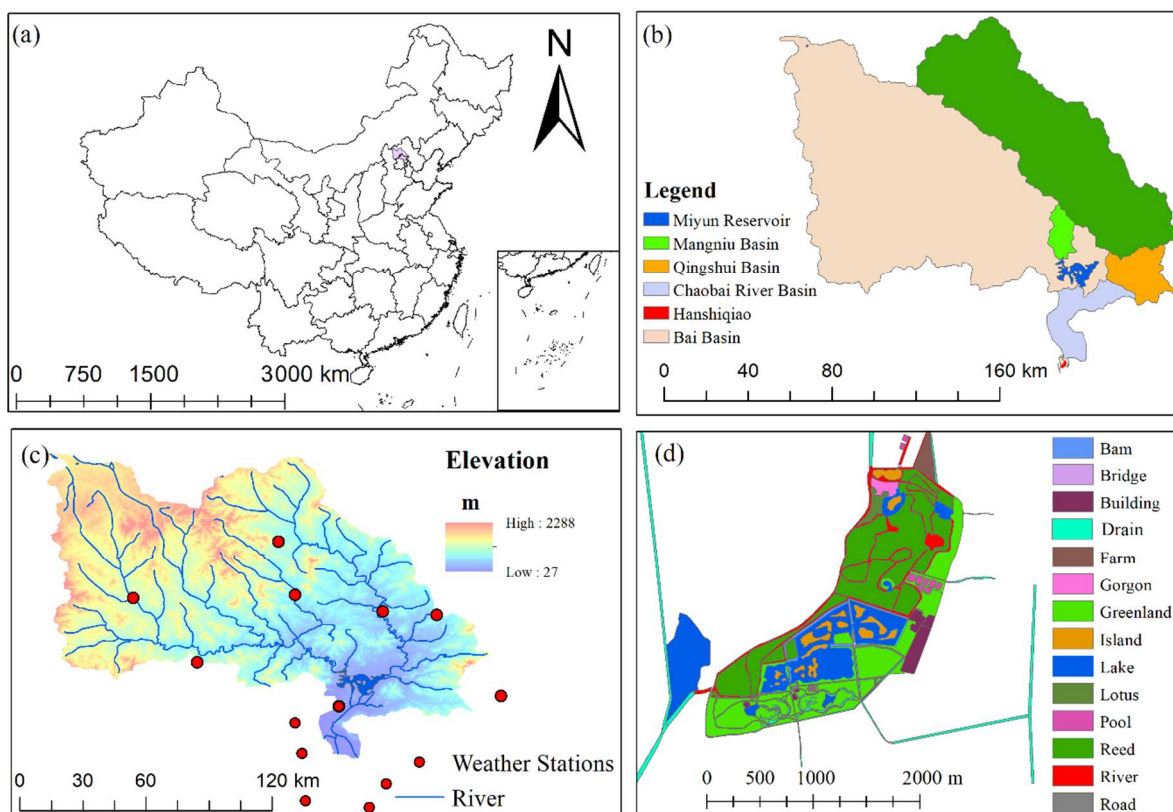


Figure 1. (a) The location of Hanshiqiao Wetland in China; (b) the Upstream River Basin of Hanshiqiao Basin; (c) the terrain of the upstream river basin of Hanshiqiao Basin and the weather stations used in this study; (d) the land use/cover of Hanshiqiao Wetland in 2020.

Hanshiqiao Wetland belongs to the Chaobai River system (see Figure 1b). Caijia River, a tributary of Chaobai River, flows through Hanshiqiao Wetland, and a primary stream flows into the wetland in average years (see Figure 1d). It is the primary source of the Hanshiqiao water area. The wetland is located in the alluvial fan of Chaobai River, belonging to the temperate and semi-humid continental monsoon climate [33]. The precipitation in the wetland area is moderate, concentrated in 6.8 months, which makes it easy for surface runoff to form, leading to good conditions for the formation of the wetland [34]. Due to the higher terrain on the south, north, and east sides of the periphery, rainwater and groundwater flow from three sides to the west depression, forming a water-collecting area. For this reason, the region has historically been hit by floods [35].

The groundwater in Hanshiqiao Wetland is quaternary unconsolidated sedimentary interstitial water. The groundwater reserves are 15–20 million m^3/km^2 . Groundwater is mainly replenished by upstream groundwater lateral runoff and infiltration of precipitation, followed by surface water seepage, irrigation water regression, etc. Stagnant water is generally distributed at the depth of 3–6 m, the water level is very shallow, and the water flow in the low-lying areas of the ground is poor. Loess clay–sand soil permeability is lacking in the formation of marsh wetlands. The annual average precipitation in Beijing is only 450 mm, and the yearly drop in groundwater level is about 1–3 m. The decline of the groundwater level in northern Shunyi and other upstream areas is more than 3 m. In addition, due to the increasing urban population and the acceleration of urban construction, the water's surface is shrinking, allowing xerophytes to invade [28,30].

Due to a lack of protection for a long time, Hanshiqiao Wetland has degraded [34]. In 2005, after establishing the Hanshiqiao Wetland Nature Reserve, they carried out several restoration measures for the wetland. The wetland restoration process mainly includes three aspects: First, they widen and clean the river, which improves the connectivity of the river; secondly, they take the farmland and aquaculture ponds back and transform

them into wetlands; and third, they build a sewage processing plant to collect sewage from nearby towns, replenish it, and recharge it into the wetland.

2.2. Dataset

This paper selected high-resolution satellite remote sensing data of Hanshiqiao Wetland Reserve in each season of 2005, 2007, 2009, 2011, 2014, and 2020 as the primary data source basically without cloud interference. More detailed information is shown in Table 1 and Figure 2. We preprocessed the images, including atmospheric correction, geometric correction, and so on. In addition, we interpreted the main land-use types of the remote sensing images using the supervised classification method and then refined the results through visual interpretation. According to the research purpose and the characteristics of Hanshiqiao Wetland, the land cover of the study area was classified into four types: lake, reed, river, and green land/building land. To ensure the accuracy of the study, the local missed pixels were manually modified with the valid image as the reference. Finally, we obtained the map of land cover for Hanshiqiao Wetland. The accuracy was verified by using the field observation data of the same period, and the accuracy of all six classification images was above 95%.

Table 1. Detailed information of the high-resolution images used in the study.

Year	Satellite	Resolution	Passing Time
2005	Quickbird	0.6 m	10.3
2007	Quickbird	0.6 m	6.20
2009	GeoEye1	0.6 m	6.20
2011	GeoEye1	0.6 m	07.3
2014	WorldView-2	0.5 m	10.17
2020	GeoEye2	0.5 m	6.14

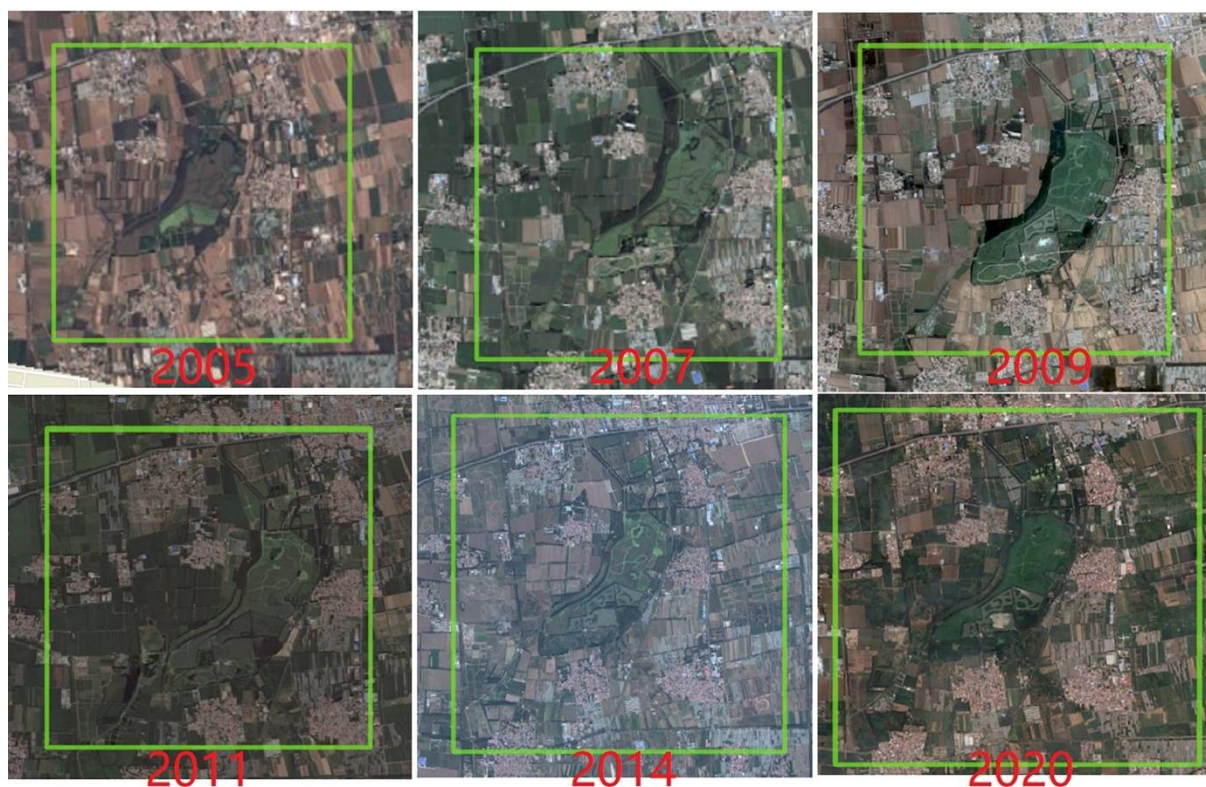


Figure 2. The screenshot of satellite images used in this study.

The China Meteorological Data Sharing Service System provides meteorological records from weather stations located in Hanshiqiao Wetland and its upstream basin (see

Figure 1c, <http://data.cma.cn/data/cdcdetail/dataCode.html>, (accessed on 4 March 2021)). The observations include air temperature, precipitation, wind speed, relative humidity, and sunshine duration. Based on the above meteorological variables, the evapotranspiration (ET) over the study regions was estimated by the Penman–Monteith equation provided by the Food and Agriculture Organization (FAO), Rome, Italy [36]. Previous studies have proven that the ET calculated by the Penman–Monteith equation agrees well with the actual evapotranspiration in Beijing, which is used to evaluate other methods [37,38]. The daily inflows and outflows of Miyun Reservoir were obtained from the Beijing Water Bureau, Beijing, China (<http://nsbd.swj.beijing.gov.cn/>, (accessed on 2 March 2021)). All the meteorological and hydrological datasets have gone through strict quality verification [39,40].

The land-use/cover dataset was obtained from the Resource and Environment Science and Data Center (<https://www.resdc.cn/>, (accessed on 13 March 2021)). The Landsat images were interpreted by human–computer interaction and transformed into the land-use/cover maps with 30 m spatial resolution. This dataset includes 6 level-1 classes (cropland, forest, grassland, water, built-up area, and barren) and the overall accuracy was reported to be higher than 94.3% [41]. Here, we selected the land-use/cover maps from 2000 and 2020 to study the land-use change in Hanshiqiao and its upstream basin.

2.3. Methods

2.3.1. IIC and PC

We used the IIC and PC to evaluate the overall connectivity of wetlands. According to previous studies and patch buffer changes, we set the resistance distance threshold of patch connectivity as 0.5 m [42–44]. To make the PC results comparable to IIC, we set connection probability as 0.5. Finally, the IIC and PC indexes were calculated by the Conefor 26 software.

$$IIC = \frac{\sum_{i=1}^n \sum_{j=1}^n a_i a_j / (1 + nl_{ij})}{A_L^2} \quad (1)$$

$$PC = \frac{\sum_{i=1}^n \sum_{j=1}^n a_i a_j p_{ij}^*}{A_L^2} \quad (2)$$

p_{ij} is the maximum product of the probability of all nodes between node i and node j . nl_{ij} is the number of shortest paths between node i and node j ; a_i and a_j are the attributes of nodes i and j , respectively (area, flow, etc.); and A_L^2 is the square of the sum of all nodes' areas. The larger the value, the better the node connectivity. Both IIC and PC have values between 0 and 1. The distance resistance threshold refers to the critical value of connection within the selected distance between two patches; if the distance between two patches exceeds the threshold, it means no contact. The greater the distance threshold, the greater the connectivity index calculated.

2.3.2. MSPA

MSPA, based on the principle of mathematical morphology and relying on basic morphological operations such as corrosion, expansion, opening, and closing, divides the foreground pixels of raffle binary images into seven mutually exclusive types: core, island, edge, perforation, bridge, circle, and branch, as shown in Figure 3 [23,45]. According to the definitions and characteristics of different MSPA landscape types, we judged the indicative signs of these landscape classifications in terms of wetland connectivity [45–47].

We extracted the water area part from the land-use map for Hanshiqiao Wetland in different periods as the foreground of MSPA analysis and other factors as the background. Considering the buffer range between dry and wet periods of wetland, we set the edge width as one pixel (i.e., 1 m). The pixel size was one meter, and an 8-neighbourhood algorithm was adopted.

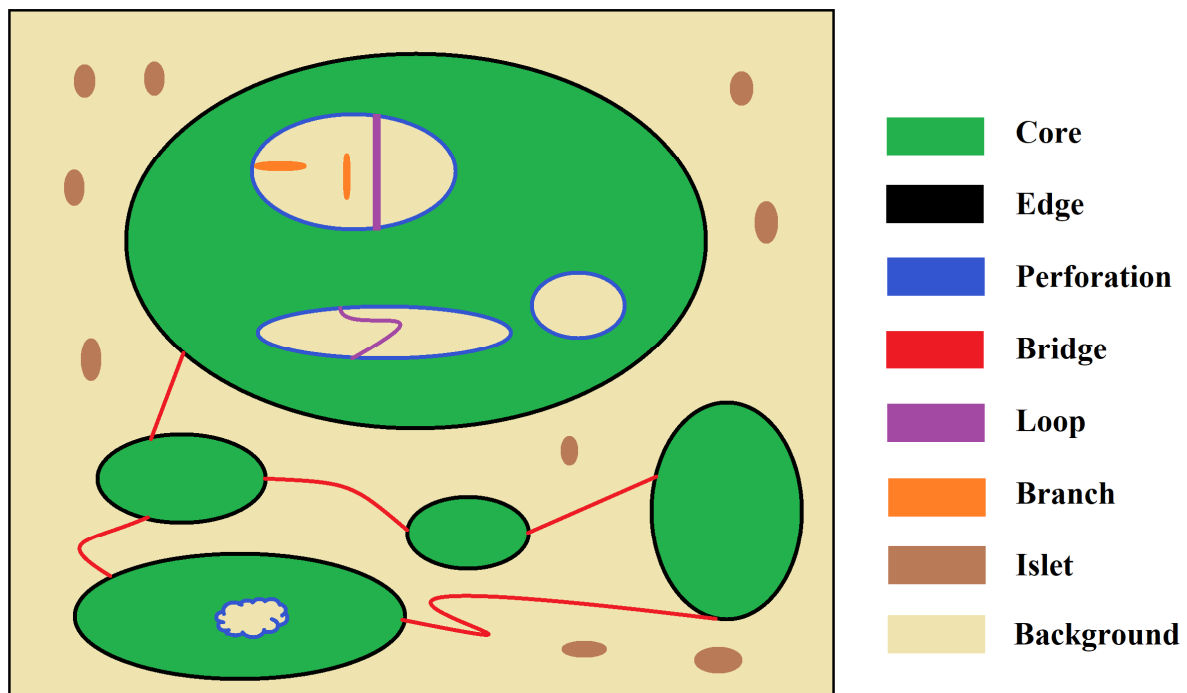


Figure 3. An illustration of the definition of the seven fragmentation classes resulting from the MSPA analysis for a hypothetical area and foreground (water) patches. Note that “Background” represents the background (non-water) areas, which are not the fragmentation classes for MSPA analysis.

2.3.3. Grey Relational Analysis (GRA)

Grey relational analysis is an effective model of grey theory to evaluate the effect of driving factors on the target variable [48]. It has drawn more and more researchers’ attention in recent years and achieved many research results [49–51]. The main procedure of GRA is firstly translating all related driving factors into comparable sequences and the target variables into reference sequences. Then, the grey relational coefficient is calculated between all comparable sequences and the reference sequence. Finally, the grey relational degree between target and comparable sequences is calculated based on these grey relational coefficients. If a comparable sequence translated from a driving factor has the highest grey relational degree between the reference sequence and itself, then the driving factor has the largest effect on changes to the target variable.

First, assuming that the value of the target variable at time t is $Z_0(t)$, the reference sequence can be constructed based on multiple samples, as shown below:

$$Z_0(t) = \{Z_0(1), Z_0(2), \dots, Z_0(t)\}; t = 1, 2, \dots, n \quad (3)$$

We may need to study multiple driving factors at the same time. Suppose we need to study M driving factors, and the value of the i th driving factor at time t is $Z_i(t)$. The comparison sequence can be expressed as:

$$Z_i(t) = \{Z_i(1), Z_i(2), \dots, Z_i(t)\}; t = 1, 2, \dots, n; i = 1, 2, \dots, m \quad (4)$$

These sequences have different physical meanings and dimensions. If the original data are used directly in GRA, the analysis result will amplify the effect of the variable with a larger value and underestimate the effect of those with a lower value. Therefore, we need to eliminate their dimensions and transform them into dimensionless data. Firstly, we

standardize all sequences by z-score standardization and the normalized sample values of $Z_0(t)$ and $Z_i(t)$ are expressed as $X_0(t)$ and $X_i(t)$, respectively:

$$X_0(t) = \frac{Z_0(t) - \mu_0}{\sigma_0} \text{ and } X_i(t) = \frac{Z_i(t) - \mu_i}{\sigma_i} \quad (5)$$

where μ and σ denotes the mean value and standard deviation of $Z_i(t)$, respectively. Then, we can calculate the grey correlation coefficient $\theta_i(t)$ between $X_0(t)$ and $X_i(t)$ with the following formula:

$$\theta_i(t) = \frac{\min(\min|X_0(t) - X_i(t)|) + \rho \max(\max|X_0(t) - X_i(t)|)}{|X_0(t) - X_i(t)| + \rho \max(\max|X_0(t) - X_i(t)|)} \quad (6)$$

The grey correlation coefficient stands for the correlation between the target sequence and the comparable sequence. It also indicates the comparable sequence's degree of influence exerted on the reference sequence. Therefore, if a comparable sequence is more important than the other one to the reference sequence, the grey correlation coefficient of this comparable sequence will be greater than others. If the two sequences are identically coincidental, the value of the grey relational grade equals 1.

For the statistical analyses, the long-term trends of variables were evaluated by linear regression. The Mann–Kendall test was performed for the statistical significance of trends, and 95% confidence intervals were provided for all trends [52,53].

3. Results

3.1. Changes in Hydrological Connectivity Based on the Connectivity Index from 2005 to 2020

From the perspective of the time change, both the PC and IIC values of Hanshiqiao water bodies showed an increasing trend (see Figure 4). The hydrological connectivity was the highest in 2020, followed by 2016. The water connectivity was the worst in 2005. The connectivity index saw the most significant increase between 2005 and 2009 due to the conversion of farmland and aquaculture ponds into lakes within Hanshiqiao Wetland.

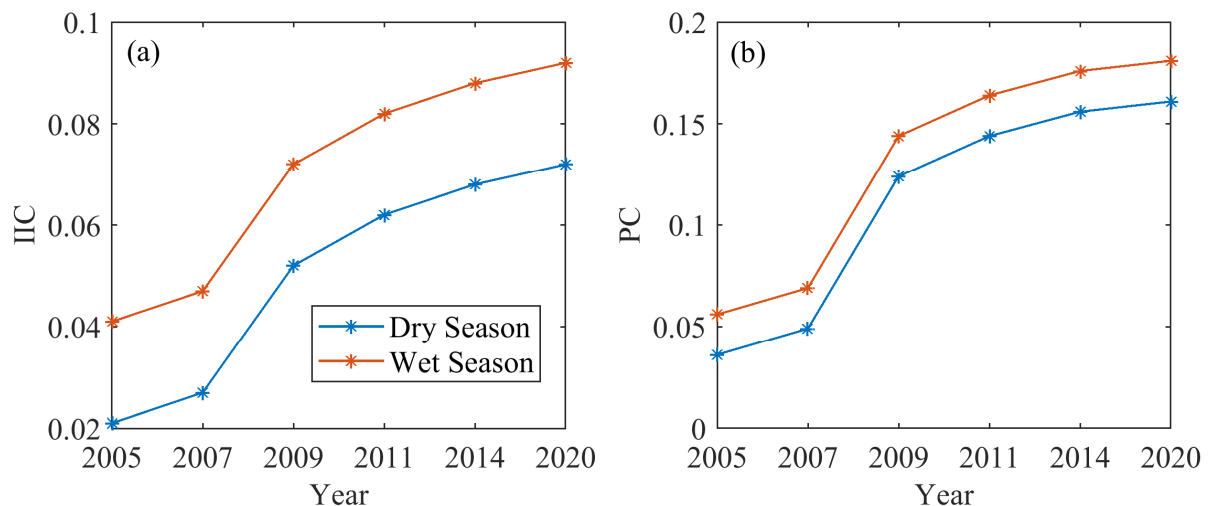


Figure 4. Integral index of connectivity (IIC, (a)) and probability of connectivity (PC, (b)) changes in Hanshiqiao Wetland in the dry season and wet season from 2005 to 2020.

3.2. Changes in Hydrological Connectivity Based on MSPA from 1990 to 2015

As shown in Figure 5, the river network of Hanshiqiao changed significantly from 2005 to 2020. Using MSPA analysis, we obtained the hydrological connectivity function pattern of Hanshiqiao Wetland in each period (see Figure 6) and the statistical table of the area (see Table 2).

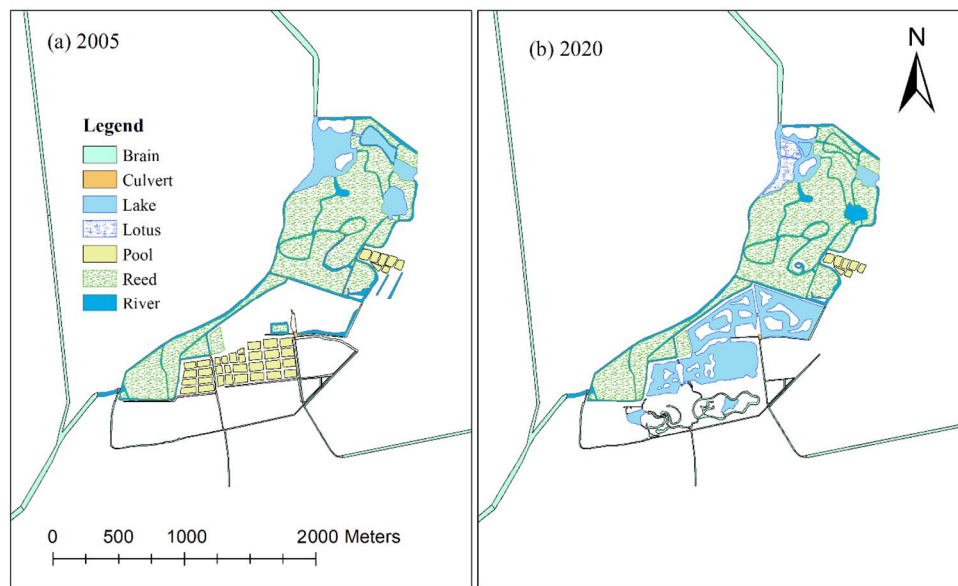


Figure 5. Changes to the Hanshiqiao Wetland ecological water system network, (a) distribution map of the Hanshiqiao Wetland ecological water system network in 2005; (b) ecological water network distribution map of Hanshiqiao Wetland in 2020.

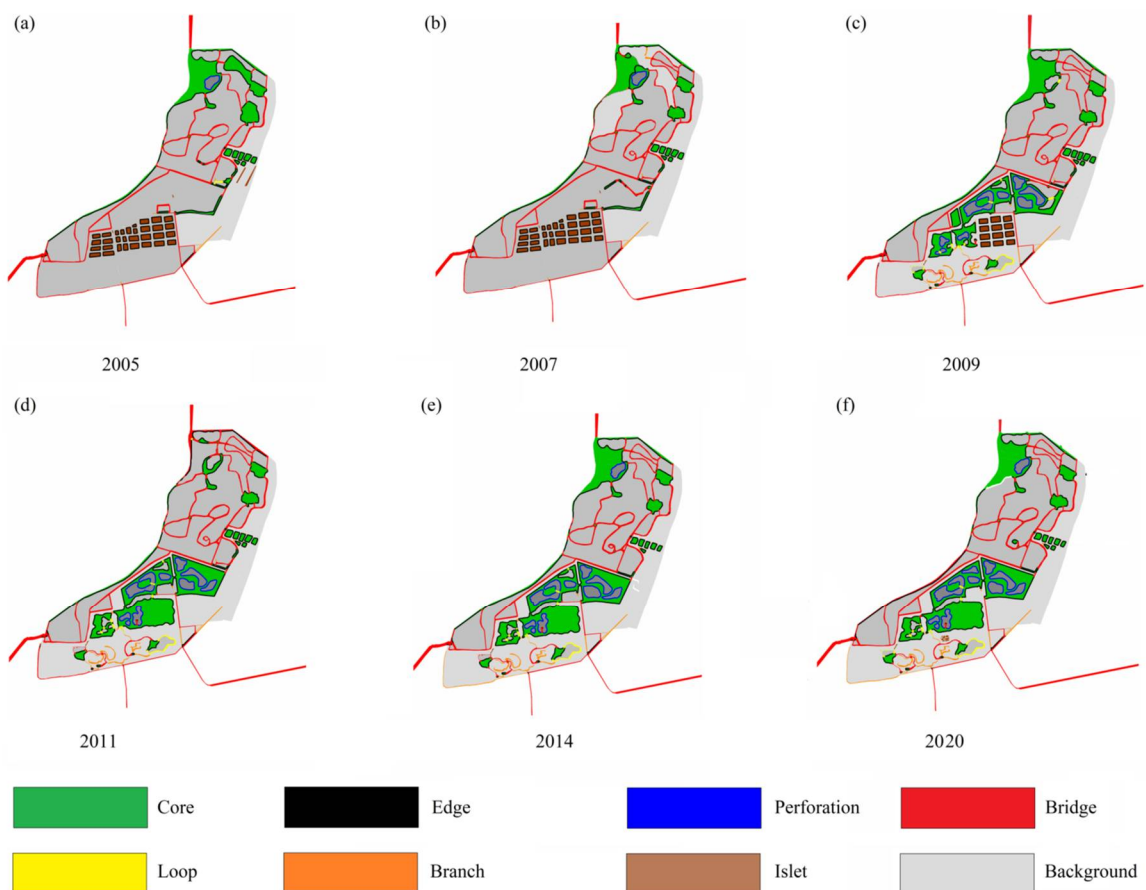


Figure 6. Pattern classes change in the study area based on MSPA from 2005 to 2020. (a–f) show the pattern of classes of Hanshiqiao Wetland in 2005, 2007, 2009, 2011, 2014, and 2020, respectively.

Table 2. Area of each MSPA class in Hanshiqiao Wetland from 2005 to 2020, units: m².

Type	2005	2007	2009	2011	2014	2020
Core	329,681	378,800	836,726	931,703	1,119,637	1,194,745
Islet	474,912	439,127	258,741	6843	5294	4779
Perforation	59,321	53,194	51,270	49,480	48,921	47,712
Edge	79,175	94,318	126,373	164,673	15,451	159,836
Loop	12,967	12,967	12,967	12,967	12,967	8967
Bridge	95,041	126,738	15,959	181,697	186,321	185,045
Branch	37,893	35,307	29,893	25,698	24,470	24,984
Background	1,347,210	1,295,749	1,104,271	1,063,139	1,023,139	923,139

Core wetland is a large habitat patch in the foreground wetland and plays the role of ecological source in wetland connectivity function. An increase in its area and fragmentation usually leads to an increase in connectivity. Edge wetland refers to the transition zone between core wetland and non-water area, which is characterized by abundant material and energy exchange. The results showed that from 2005 to 2020, the core wetland and marginal wetland showed an adverse area change trend. The core wetland increased in the early stage and tended to stabilize after 2014. From 2005 to 2020, the proportion of core area increased first and then kept stable, whereas that of the edge area decreased in terms of space and area. The core wetland showed the characteristics of gradual fragmentation and recovery from 2005 to 2020. Combined with the changes in wetland hydrological connectivity, it can also be seen that the change in core wetland plays a leading role in its recovery.

Branches, bridges, and loops all play the role of a corridor in wetland connectivity. In the wetland hydrological landscape, bridges are mainly manifested as large river channels and ditches, which are the channels connecting two different core patches. Branches represent the connection between the core wetland and other hydrological landscapes of wetland. They are the channels for species diffusion and energy exchange between the core patch and its peripheral hydrological patch. In wetland hydrological landscape, branches mainly consists of large lakes, rivers, and ditches. A loop is a shortcut for the inner connection of the core patches, which is conducive to the internal link of the core wetland. Among the three types of hydrological patch, bridges contributed the most to hydrological connectivity, followed by branches, and loops contributed the least. From 2005 to 2020, the area of the bridge and roundabout increased significantly, whereas the area of the branch decreased significantly. The rise of the bridge wetland was mainly due to the dredging of natural river channels and the construction of artificial ditches. The increase in loop wetland was primarily due to the construction of several central islands in the lake after transforming farmland and cropland into lakes (see Figure 5b,c). However, with the continuous expansion of the core wetland area, the actual branch wetland gradually integrated into the core area, so the area of the branch wetland gradually decreased. Because core wetlands play a leading role in wetland hydrological connectivity, the conversion of branch wetlands into core wetlands increased the hydrological connectivity of the wetland. Therefore, the area change in the three wetland types plays an essential role in promoting hydrological connectivity (see Figure 7).

An islet is a small patch with little interconnection, mainly including small puddles, ponds, and breeding pools in the wetland. However, there is less possibility for matter and energy inside the islet wetlands to communicate with the outside world. The transformation of an islet into core wetland is helpful to improve the hydrological connectivity of Hanshiqiao Wetland. From 2005 to 2020, the total area of the islet decreased by 99.0%. The reduction in islets was mainly due to the conversion of small aquaculture ponds into lakes. Perforation patches showed a slight decreasing trend. However, the ratio of perforation type in the foreground was the smallest, and the maximum was not more than 2.43%, which had little impact on the hydrological connectivity of Hanshiqiao Wetland.

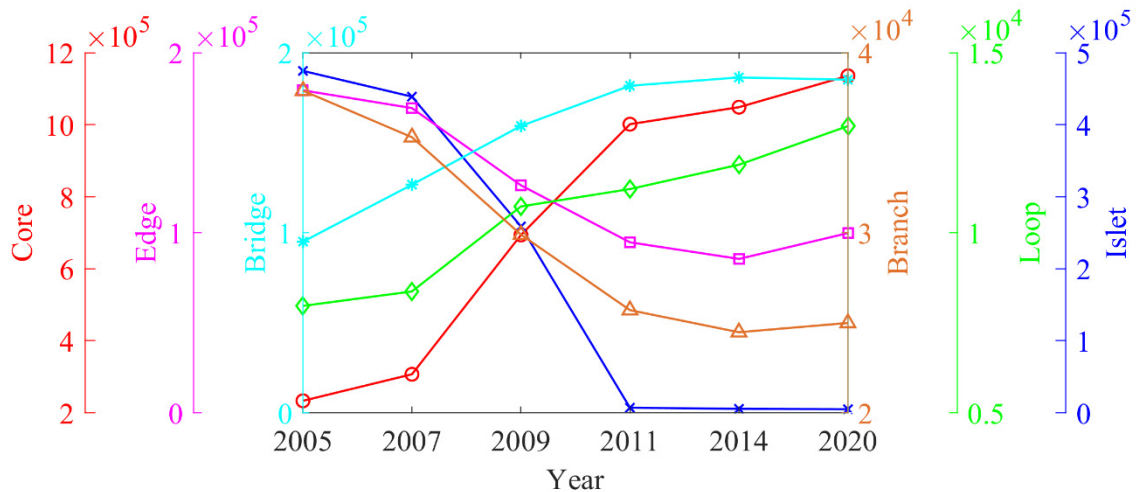


Figure 7. The change in the area of patch classes for Hanshiqiao Wetland during 2005–2020, unit: m².

3.3. Spatial Pattern Evolution of Hydrological Connectivity

Based on the connectivity index and MSPA model, the spatial evolution of hydrological connectivity in Hanshiqiao Wetland from 2005 to 2020 was divided into two stages: restoration and stabilization.

Hydrological connectivity recovery stage (2005–2011): (1) The area and number of core wetlands gradually increased, and the proportion of core wetlands gradually increased. The morphology developed from elongated to saturated. (2) Islet patches were gradually absorbed by the saturated core patch. Branch wetland integrated into core wetlands. (3) The area and number of islets decreased and transformed into core patches. (4) The area of both perforation and edge patches gradually decreased, and their proportion of the total area of Hanshiqiao Wetland Reserve decreased obviously.

Hydrological connectivity stabilization stage (2011–2020): In the stable period, the area of different types of wetland in Hanshiqiao remained unchanged. The critical factor affecting the hydrological connectivity of Hanshiqiao Wetland was no longer the patch type change but the wetland's water level changes. The water level of wetland patches are relatively shallow, especially in some artificial channels and silted waterways. When the water level rises, submerged reed wetlands and tidal flats can significantly increase the hydrological connectivity of wetlands. Reduced hydrology can lead to river interruption, and these bridge wetlands can become branch wetlands or dry land. The reduction of the bridge class makes the wetland patches connect TO the core wetland through the bridge wetland, becoming an island wetland. Therefore, after 2011, increasing the water level of Hanshiqiao Wetland was a critical factor to maintain and improve the hydrological connectivity of Hanshiqiao Wetland.

3.4. Driving Factors of Hydrological Connectivity Change in Hanshiqiao Wetland

3.4.1. Truncation of Water from Upstream Water Conservancy Projects Leads to Reduction of Water Reserves

The core wetland area plays a significant role in determining the hydrological connectivity of Hanshiqiao Wetland. However, Miyun Reservoir and other water conservancy facilities have been built on the main recharge river upstream of Hanshiqiao Wetland to intercept most of the inflow (see Figure 1b,c). Miyun Reservoir is one of the most critical water sources in Beijing. As the city grew and the population exploded, Miyun Reservoir intercepted more water and stopped releasing water downstream most of the time. As a result, much of the downstream river, including the Caijia River (see Figure 1d), has been cut off for years. Besides reservoirs, upland water has been extracted for agricultural irrigation, urban production, and living water. According to relevant data, except for the flood season in a few years, there is almost no water flowing into Hanshiqiao Wetland

through the Caijia River. To solve the long-term water shortage problem in Hanshiqiao Wetland, after 2009, Hanshiqiao Wetland Nature Reserve Management Center organized the construction of the Yangzhen Sewage Treatment Plant. The sewage treatment plant is mainly used to collect the sewage generated by the surrounding cities, villages, and enterprises. After purification, the generated reclaimed water is injected into Hanshiqiao Wetland through the Jiajia River (see Figure 1d). This water has become a key factor controlling the formation and development of wetland vegetation and soil, especially in dry seasons. Hanshiqiao Wetland connectivity and corresponding ecological function have been restored with a stable water supply.

3.4.2. Impacts of Land-Use Changes on Wetland Connectivity

Land-use changes are closely related to social and economic development and significantly impact the wetland ecosystem in Hanshiqiao. We mainly focus on two aspects of land-use change characteristics. The first is the land-use change in Hanshiqiao Wetland affecting the wetland's hydrological connectivity by changing the wetland's landscape pattern. The other is the land-use change in the upstream basin of Hanshiqiao Wetland. The evolution of land use in the upstream basin can change the water cycle process, thus affecting water inflow to Hanshiqiao Wetland. Land-use changes within Hanshiqiao Wetland are analyzed in Section 3.3. With the continuous implementation of the wetland protection project, the area of the core wetland inside Hanshiqiao is increasing. Additionally, with the deepening of river dredging and the construction of artificial ditches, land-use changes in Hanshiqiao Wetland from 2005 to 2020 significantly increased the hydrological connectivity of Hanshiqiao Wetland.

According to land-use maps from 2005 and 2020 (see Figure 8 and Table 3), buildings had the most significant increase in the upstream basin of Hanshiqiao Wetland, which increased by 3.31 times during this period. The new buildings were mainly concentrated in the Chaobai River section between Miyun Reservoir and Hanshiqiao Wetland (see Figure 8). The increased buildings primarily came from the cropland, accounting for 66.1% of the new area. The forest area increased by 176.7 km² during the study period, mainly transferred from grassland and cropland. The expansion of buildings and forests has also led to a sharp increase in water consumption. The water source was mainly provided by groundwater and the upstream river for industrial, agricultural, and residential use. The increasing forest leads to increased water consumption and storage capacity, making it difficult for general precipitation to form adequate surface runoff and reducing the efficiency of reservoir water replenishment [54,55]. Those land-use changes made it difficult for Hanshiqiao Wetland to obtain water to increase effective hydrological connectivity. Note that our land-use classification is relatively simple, unable to explore some more complicated problems. For example, the native forest of the basin water cycle and nutrition change significantly differ from the exotic forest in hydrological sediments and nutrients [56,57]. However, we still cannot effectively distinguish them now and hope to explore this problem in the future.

Table 3. Transition matrix of land use/land cover for the upstream basin of Hanshiqiao Wetland from 2005 to 2020, units: km².

		2020						
		Cropland	Forest	Grassland	Wetland	Buildings	Bare Land	Total
2005	Cropland	4224.0	289.8	376.8	33.1	248.1	9.0	5198.0
	Forest	235.1	13,960.1	1202.2	13.5	34.2	7.8	15,495.8
	Grassland	521.7	1361.6	6636.2	21.4	93.8	21.0	8667.0
	Wetland	45.6	19.4	16.6	204.5	11.8	2.1	301.3
	Building	5.4	2.9	2.6	5.7	154.2	0.4	175.6
	Bare land	3.0	0.4	0.5	0.4	0.9	7.1	12.6
	Total	5036.5	15,672.5	8236.1	279.8	550.9	47.7	29,864.4

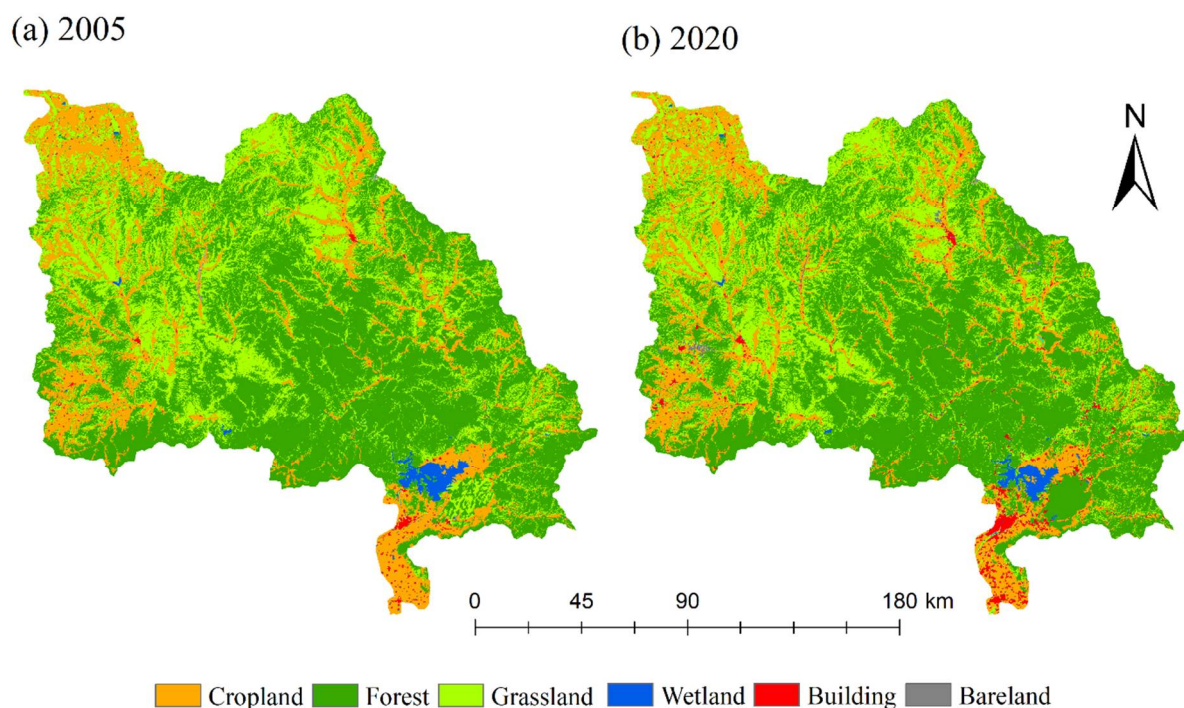


Figure 8. (a,b) show the landscape type maps of the upstream river basin for Hanshiqiao Wetland in 2005 and 2020, respectively.

3.4.3. Impacts of Climate Change on Wetland Connectivity

The impact of climate change on wetland connectivity in Hanshiqiao Wetland is long term and slow. Climate change usually affects the landscape pattern of wetlands, including the hydrological connectivity of wetlands. Wetland systems are particularly vulnerable to climate change, especially in arid areas, which threaten the continued existence of wetlands. From 2005 to 2020, the air temperature showed a significant increasing trend in both Hanshiqiao Wetland and its upstream watershed (see Figure 8a,c). The annual precipitation had no significant long-term trend but had a sharp decrease after 1998 (see Figure 9b,d). In addition, the reduction of wind speed and sunshine duration indicated that the potential evapotranspiration of both Hanshiqiao Wetland and upstream basin showed a downward trend. This result was consistent with the long-term trend of station-observed evapotranspiration. The warming and drying of regional climate caused by rising temperature and decreasing precipitation decrease incoming water from the upstream reaches of Hanshiqiao Wetland. Therefore, overall, climate change may exacerbate the water shortage in Hanshiqiao Wetland.

3.4.4. Grey Relational Analysis of Driving Factors and Wetland Connectivity

Here, we want to evaluate the impacts of reservoir construction, land-use change, and climate change on the hydrological connectivity of Hanshiqiao Wetland. Therefore, we took the IIC/PC as the reference sequences on behalf of the changes in hydrological connectivity. Based on the above analysis, we used the water releases from Miyun Reservoir, the proportion of forest and build-up area, air temperature, precipitation, and evapotranspiration as comparable sequences. Then, we evaluated their effect on the hydrological connectivity by grey relational analysis (see Section 3.4.4).

As shown in Table 4, the outflow of Miyun Reservoir is most closely related to the hydrological connectivity of Hanshiqiao Wetland. The upstream drainage can directly recharge Hanshiqiao Wetland and raise the water level of Hanshiqiao Wetland, thus improving the hydrological connectivity of the wetland. The precipitation in Hanshiqiao Basin is mainly concentrated in summer, so the water level in winter is mainly maintained

by runoff from upstream. Therefore, in Hanshiqiao Wetland, the hydrological connectivity is more sensitive to outflow from Miyun Reservoir in cold seasons than in warm seasons.

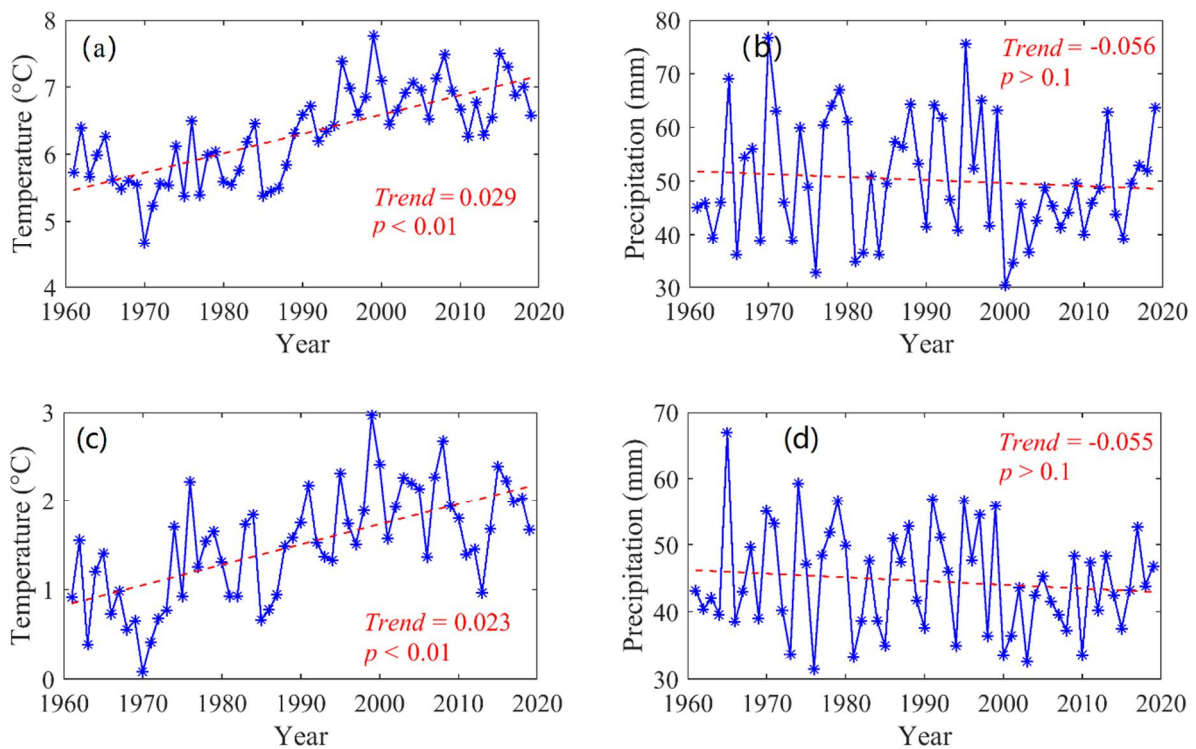


Figure 9. The temperature and precipitation changes for Hanshiqiao Wetland (a,b) and its upstream watershed (c,d) during 1960–2020. The trend denotes the temperature and precipitation trend, and p represents the p -value for the significance test for trends.

Table 4. The grey correlation coefficients between the IIC/PC and driving factors.

		Reservoir	Land-Use Change		Climate Change		
		Water Release	Forest	Urban	Temperature	Precipitation	ET
IIC	All year	0.857	0.654	0.637	0.574	0.849	0.731
	Warm	0.823	0.741	0.558	0.522	0.894	0.836
	Cold	0.916	0.592	0.715	0.597	0.798	0.645
PC	All year	0.861	0.661	0.643	0.581	0.841	0.729
	Warm	0.839	0.764	0.561	0.530	0.890	0.841
	Cold	0.928	0.607	0.709	0.614	0.803	0.652

The impact of climate change is second only to the outflow of the upstream reservoir. Climate change mainly affects the hydrological connectivity of Hanshiqiao Wetland by changing regional precipitation and evapotranspiration (see Table 4). The precipitation in Hanshiqiao watershed can continuously confluence to Hanshiqiao Wetland through the surrounding artificial ditches, which become one of the most important recharge water sources for the wetland. The precipitation in this region is mainly concentrated in the warm season; thus, the precipitation and IIC/PC relationship are closer in the warm seasons than in the cold seasons. In addition, to maintain the water level, a dam was built at the outlet of Hanshiqiao Wetland. As a result, the outflow of Hanshiqiao Wetland is very low and most of the water is consumed through evapotranspiration. Therefore, evapotranspiration is also a key factor affecting the hydrological connectivity of Hanshiqiao Wetland, which has a larger grey correlation coefficient with the IIC and PC. Compared with precipitation and evapotranspiration, the air temperature has a lower grey correlation efficient with the IIC/PC. The air temperature does not directly affect the water level of Hanshiqiao Wetland but does affect evapotranspiration. Besides air temperature, evapotranspiration

is also affected by other factors such as wind speed, which may be why air temperature may have a more negligible effect on hydrological connectivity than precipitation and evapotranspiration [58,59].

The land-use/cover changes in the upper reaches of Hanshiqiao Wetland also has a specific influence on the hydrological connection of Hanshiqiao Basin. The grey correlation coefficients between forestland and urban area changed and the IIC (PC) were 0.654 (0.661) and 0.637 (0.643), respectively. The increase in forest area can trap more precipitation for evapotranspiration, thus reducing the runoff depth of the upper reaches of Hanshiqiao Wetland. Urbanization increases domestic, industrial, and agricultural water and reduces the groundwater level and upstream inflow of Hanshiqiao Wetland. The city's water consumption should be much higher than that of the forestland, and it should have a more significant impact on the hydrological connectivity of Hanshiqiao Wetland. However, the increase in the impervious surface caused by urbanization can increase the surface confluence, thus enhancing the replenishment of precipitation in Hanshiqiao Wetland and offsetting part of the impact caused by the increase in urban water consumption. Additionally, the sewage treatment plant in Yangzhen (located in the upper reaches of the Jiajia River, see Figure 1d) replenishes Hanshiqiao Wetland by purifying the collected urban sewage, reducing the impact of urbanization on the hydrological connectivity.

4. Summary and Conclusions

Combining mathematical morphology and the Connectivity Index, this paper reveals the process of changes in hydrological connectivity at the landscape and pixel levels. It summarizes the spatial morphological evolution mechanism and driving factors of wetland hydrological connectivity in Hanshiqiao Wetland.

(1) Based on the connectivity index, the hydrological connectivity of Hanshiqiao Wetland significantly increased from 2005 to 2011 and tended to be stable after 2011.

(2) Based on the MSPA model, the spatial morphology of Hanshiqiao Wetland was divided into seven types: core, island, edge, perforation, bridge, circle, and branch. According to the comprehensive change characteristics of each type, the spatial morphological evolution of the hydrological connectivity of Hanshiqiao Wetland was divided into two stages: the recovery stage and the stable stage. In the recovery stage, the branches and islets gradually merged into core patches, and the area of both bridge and loop increased substantially. In the stable stage, the area composition of the wetland landscape gradually tended to be stable. The water level plays a leading role in changing the hydrological connectivity of Hanshiqiao Wetland.

(3) Based on the grey correlation analysis, the main driving factors for the change in the hydrological connectivity of Hanshiqiao Wetland are as follows: Miyun Reservoir intercepts most of the incoming water, resulting in a significant reduction in upstream recharge water; reduced precipitation and enhanced evapotranspiration have exacerbated drought in the region; and the expansion of forest and urbanization aggravate the water shortage of the upstream watershed, further reducing the inflow into Hanshiqiao Wetland.

According to the classification principle of MSPA and existing research results, pixel size has a significant impact on the landscape classification results of MSPA [43]. Many pixels will lead to some core areas being classified as other types. Based on high-resolution remote sensing images with a resolution of more than 1 m, the water body of Hanshiqiao Wetland is divided into seven morphological types, and the hydrological connectivity of Hanshiqiao Wetland is mainly evaluated overall. Still, the connectivity function of some small areas is not discussed. For example, an islet wetland is equivalent to an "ecological jump island" in the ecological network, which can provide temporary habitat for species such as water birds and play the role of ecological media in the ecological function. However, connectivity analysis based on the MSPA model and the Connectivity Index often ignores the connectivity function of islet wetlands. It emphasizes the decrease in overall connectivity caused by the increase in patch number. Therefore, future research can be compared with multiple scales. The influence of different scales on connectivity

change and the spatial morphological evolution mechanism needs to be further studied and combined with the ecological service function of wetland type. Based on the value of ecological services, a more comprehensive evaluation system of connectivity function can be established for each landscape type.

According to the morphological evolution mechanism of wetlands, wetland protection should avoid wetland fragmentation primarily to ensure the integrity of the core wetland. During the restoration of degraded wetlands, islet wetlands should be reduced as much as possible or incorporated into core wetlands through the repair and construction of corridor wetlands. More importantly, due to climate change and human activities, the natural water supply of Hanshiqiao Wetland will become even more scarce in the future. Therefore, it is necessary to provide a reliable water source for the ecological water demand of Hanshiqiao Wetland by increasing sewage treatment and watershed water diversion.

Author Contributions: Data curation, Y.Z.; Resources, B.C. (Bao Cao); Supervision, B.C. (Baoshan Cui); Writing—original draft, Q.Z.; Writing—review & editing, S.C. and J.D. All authors have read and agreed to the published version of the manuscript.

Funding: This study was funded by the National Basic Research Program of China (2018YFC1507701), the National Natural Science Foundation of China (42005019), and Major science and technology R&D project of Shunyi District, Beijing, China.

Institutional Review Board Statement: Not applicable.

Informed Consent Statement: Not applicable.

Data Availability Statement: Not applicable.

Conflicts of Interest: The authors declare no conflict of interest.

References

1. Cohen, M.J.; Creed, I.F.; Alexander, L.; Basu, N.B.; Calhoun, A.J.K.; Craft, C.; D’Amico, E.; DeKeyser, E.; Fowler, L.; Golden, H.E.; et al. Do geographically isolated wetlands influence landscape functions? *Proc. Natl. Acad. Sci. USA* **2016**, *113*, 1978–1986. [[CrossRef](#)] [[PubMed](#)]
2. Grill, G.; Lehner, B.; Lumsdon, A.E.; MacDonald, G.K.; Zarfl, C.; Liermann, C.R. An index-based framework for assessing patterns and trends in river fragmentation and flow regulation by global dams at multiple scales. *Environ. Res. Lett.* **2015**, *10*, 015001. [[CrossRef](#)]
3. Golden, H.E.; Creed, I.F.; Ali, G.; Basu, N.B.; Neff, B.P.; Rains, M.C.; McLaughlin, D.; Alexander, L.C.; Ameli, A.A.; Christensen, J.R.; et al. Integrating geographically isolated wetlands into land management decisions. *Front. Ecol. Environ.* **2017**, *15*, 319–327. [[CrossRef](#)] [[PubMed](#)]
4. Bracken, L.J.; Turnbull, L.; Wainwright, J.; Bogaart, P. Sediment connectivity: A framework for understanding sediment transfer at multiple scales. *Earth Surf. Process. Landforms* **2014**, *40*, 177–188. [[CrossRef](#)]
5. Fry, G.; Tveit, M.S.; Ode, A.; Velarde, M.D. The ecology of visual landscapes: Exploring the conceptual common ground of visual and ecological landscape indicators. *Ecol. Indic.* **2009**, *9*, 933–947. [[CrossRef](#)]
6. Singh, M.; Tandon, S.K.; Sinha, R. Assessment of connectivity in a water-stressed wetland (Kaabar Tal) of Kosi-Gandak interfan, north Bihar Plains, India. *Earth Surf. Process. Landforms* **2017**, *42*, 1982–1996. [[CrossRef](#)]
7. Western, A.W.; Blöschl, G.; Grayson, R.B. Toward capturing hydrologically significant connectivity in spatial patterns. *Water Resour. Res.* **2001**, *37*, 83–97. [[CrossRef](#)]
8. Pringle, C. What is hydrologic connectivity and why is it ecologically important? *Hydrol. Process.* **2003**, *17*, 2685–2689. [[CrossRef](#)]
9. Tischendorf, L.; Fahrig, L. How should we measure landscape connectivity? *Landsc. Ecol.* **2000**, *15*, 633–641. [[CrossRef](#)]
10. Lehmann, P.; Hinz, C.; McGrath, G.; Meerveld, H.J.T.-V.; McDonnell, J.J. Rainfall threshold for hillslope outflow: An emergent property of flow pathway connectivity. *Hydrol. Earth Syst. Sci.* **2007**, *11*, 1047–1063. [[CrossRef](#)]
11. Urban, D.; Keitt, T. Landscape Connectivity: A Graph-Theoretic Perspective. *Ecology* **2001**, *82*, 1205–1218. [[CrossRef](#)]
12. Cui, G.; Liu, Y.; Tong, S. Analysis of the causes of wetland landscape patterns and hydrological connectivity changes in Momoge National Nature Reserve based on the Google Earth Engine Platform. *Arab. J. Geosci.* **2021**, *14*, 1–16. [[CrossRef](#)]
13. Tananaev, N.; Isaev, V.; Sergeev, D.; Kotov, P.; Komarov, O. Hydrological Connectivity in a Permafrost Tundra Landscape near Vorkuta, North-European Arctic Russia. *Hydrology* **2021**, *8*, 106. [[CrossRef](#)]
14. Bergsten, A.; Galafassi, D.; Bodin, Ö. The problem of spatial fit in social-ecological systems: Detecting mismatches between ecological connectivity and land management in an urban region. *Ecol. Soc.* **2014**, *19*, 17–39. [[CrossRef](#)]
15. Erős, T.; Olden, J.D.; Schick, R.S.; Schmera, D.; Fortin, M.-J. Characterizing connectivity relationships in freshwaters using patch-based graphs. *Landsc. Ecol.* **2011**, *27*, 303–317. [[CrossRef](#)]

16. Hermoso, V.; Ward, D.P.; Kennard, M.J. Using water residency time to enhance spatio-temporal connectivity for conservation planning in seasonally dynamic freshwater ecosystems. *J. Appl. Ecol.* **2012**, *49*, 1028–1035. [CrossRef]
17. McIntyre, N.E.; Wright, C.K.; Swain, S.; Hayhoe, K.; Liu, G.; Schwartz, F.W.; Henebry, G.M. Climate forcing of wetland landscape connectivity in the Great Plains. *Front. Ecol. Environ.* **2014**, *12*, 59–64. [CrossRef]
18. An, Y.; Liu, S.; Sun, Y.; Shi, F.; Beazley, R. Construction and optimization of an ecological network based on morphological spatial pattern analysis and circuit theory. *Landsc. Ecol.* **2020**, *36*, 2059–2076. [CrossRef]
19. Lin, J.; Huang, C.; Wen, Y.; Liu, X. An assessment framework for improving protected areas based on morphological spatial pattern analysis and graph-based indicators. *Ecol. Indic.* **2021**, *130*, 108138. [CrossRef]
20. Rogan, J.; Wright, T.; Cardille, J.; Pearsall, H.; Ogneva-Himmelberger, Y.; Riemann, R.; Riitters, K.; Partington, K. Forest fragmentation in Massachusetts, USA: A town-level assessment using Morphological spatial pattern analysis and affinity propagation. *GIScience Remote Sens.* **2016**, *53*, 506–519. [CrossRef]
21. Birk, S.; Chapman, D.; Carvalho, L.; Spears, B.M.; Andersen, H.E.; Argillier, C.; Auer, S.; Baattrup-Pedersen, A.; Banin, L.; Beklioglu, M.; et al. Impacts of multiple stressors on freshwater biota across spatial scales and ecosystems. *Nat. Ecol. Evol.* **2020**, *4*, 1060–1068. [CrossRef] [PubMed]
22. Li, Y.-Y.; Zhang, Y.-Z.; Jiang, Z.-Y.; Guo, C.-X.; Zhao, M.-Y.; Yang, Z.-G.; Guo, M.-Y.; Wu, B.-Y.; Chen, Q.-L. Integrating morphological spatial pattern analysis and the minimal cumulative resistance model to optimize urban ecological networks: A case study in Shenzhen City, China. *Ecol. Process.* **2021**, *10*, 1–15. [CrossRef]
23. Yang, R.; Bai, Z.; Shi, Z. Linking Morphological Spatial Pattern Analysis and Circuit Theory to Identify Ecological Security Pattern in the Loess Plateau: Taking Shuozhou City as an Example. *Land* **2021**, *10*, 907. [CrossRef]
24. Yang, Z.G.; Jiang, Z.Y.; Guo, C.X.; Yang, X.J.; Xu, X.J.; Li, X.; Hu, Z.M.; Zhou, H.Y. Construction of ecological network using morphological spatial pattern analysis and minimal cumulative resistance models in Guangzhou City, China. *Ying Yong Sheng Tai Xue Bao = J. Appl. Ecol.* **2018**, *29*, 3367–3376.
25. Wang, J.; Xu, C.; Pauleit, S.; Kindler, A.; Banzhaf, E. Spatial patterns of urban green infrastructure for equity: A novel exploration. *J. Clean. Prod.* **2019**, *238*, 117858. [CrossRef]
26. Song, S.; Albert, C.; Prominski, M. Exploring integrated design guidelines for urban wetland parks in China. *Urban For. Urban Green.* **2020**, *53*, 126712. [CrossRef]
27. Kumwimba, M.N.; Li, X.; Wang, W.; De Silva, L.; Bao, L.; Mihiranga, H.; Su, J.; Li, X. Large-scale hybrid accidental urban wetland for polluted river purification in northern China: Evidence and implications for urban river management. *Environ. Technol. Innov.* **2021**, *22*, 101542. [CrossRef]
28. Xia, J.; Zheng, F.; Tang, H.; Li, J.; Li, Y. Chemical speciation and risks of heavy metals in sediment of urban wetlands in southeastern China. *Soil Sediment Contam. Int. J.* **2018**, *28*, 15–27. [CrossRef]
29. Meng, W.; He, M.; Hu, B.; Mo, X.; Li, H.; Liu, B.; Wang, Z. Status of wetlands in China: A review of extent, degradation, issues and recommendations for improvement. *Ocean Coast. Manag.* **2017**, *146*, 50–59. [CrossRef]
30. Cui, L.; Zuo, X.; Dou, Z.; Huang, Y.; Zhao, X.; Zhai, X.; Lei, Y.; Li, J.; Pan, X.; Li, W. Plant identification of Beijing Hanshiqiao wetland based on hyperspectral data. *Spectrosc. Lett.* **2021**, *54*, 381–394. [CrossRef]
31. Zhang, W.; Yao, L.; Li, H.; Sun, D.; Zhou, L. Research on Land Use Change in Beijing Hanshiqiao Wetland Nature Reserve Using Remote Sensing and GIS. *Procedia Environ. Sci.* **2011**, *10*, 583–588. [CrossRef]
32. Zhao, Y.; Liu, Y.; Wu, S.; Li, Z.; Zhang, Y.; Qin, Y.; Yin, X. Construction and application of an aquatic ecological model for an emergent-macrophyte-dominated wetland: A case of Hanshiqiao wetland. *Ecol. Eng.* **2016**, *96*, 214–223. [CrossRef]
33. Zhang, J.; Chen, Y.; Lei, T.; Chen, J.; Cui, G. Inter-specific relations of the dominant plant populations in the Hanshiqiao Wetland in Beijing. *Wetl. Sci.* **2007**, *5*, 146.
34. Liu, S.; Hong, J.M.; Hu, D.; Jiang, Z.Q. Vegetation classification and the change of vegetation pattern from 2003 to 2006 in the Hanshiqiao Wetland Nature Reserve, Beijing. *Wetl. Sci.* **2008**, *6*, 19–28.
35. Zhang, J. Primary Studies on Plants and Vegetation in Hanshiqiao Wetland Nature Reserve in Beijing. Master's Thesis, Beijing Forestry University, Beijing, China, 2007; pp. 10–11. Available online: <https://kns.cnki.net/kcms/detail/detail.aspx?dbcode=CMFD&dbname=CMFD2007&filename=2007077207.nh&uniplatform=NZKPT&v=TLfYQ0ssVGVogJ5KJWhqmuuiakL2N6KHDpPUtL87mQZjwHXBQQe7r2GIUvECbWQB> (accessed on 1 June 2007).
36. Cai, J.; Liu, Y.; Lei, T.; Pereira, L.S. Estimating reference evapotranspiration with the FAO Penman–Monteith equation using daily weather forecast messages. *Agric. For. Meteorol.* **2007**, *145*, 22–35. [CrossRef]
37. Haijun, L.; Yan, L.; Ruihao, Z.; Guanhua, H. Evaluation and modification of potential evapotranspiration methods in Beijing, China. *Int. J. Agric. Biol. Eng.* **2013**, *6*, 9–18.
38. Yang, Q.; Ma, Z.; Zheng, Z.; Duan, Y. Sensitivity of potential evapotranspiration estimation to the Thornthwaite and Penman–Monteith methods in the study of global drylands. *Adv. Atmos. Sci.* **2017**, *34*, 1381–1394. [CrossRef]
39. Cao, L.; Zhu, Y.; Tang, G.; Yuan, F.; Yan, Z. Climatic warming in China according to a homogenized data set from 2419 stations. *Int. J. Climatol.* **2016**, *36*, 4384–4392. [CrossRef]
40. Du, J.; Wang, K.; Wang, J.; Ma, Q. Contributions of surface solar radiation and precipitation to the spatiotemporal patterns of surface and air warming in China from 1960 to 2003. *Atmos. Chem. Phys.* **2017**, *17*, 4931–4944. [CrossRef]
41. Liu, J.; Zhang, Z.; Xu, X.; Kuang, W.; Zhou, W.; Zhang, S.; Li, R.; Yan, C.; Yu, D.; Wu, S.; et al. Spatial patterns and driving forces of land use change in China during the early 21st century. *J. Geogr. Sci.* **2010**, *20*, 483–494. [CrossRef]

42. Saura, S.; Pascual-Hortal, L. A new habitat availability index to integrate connectivity in landscape conservation planning: Comparison with existing indices and application to a case study. *Landscape Urban Plan.* **2007**, *83*, 91–103. [[CrossRef](#)]
43. Velázquez, J.; Gutiérrez, J.; Hernando, A.; García-Abril, A. Evaluating landscape connectivity in fragmented habitats: Cantabrian capercaillie (*Tetrao urogallus cantabricus*) in northern Spain. *For. Ecol. Manag.* **2017**, *389*, 59–67. [[CrossRef](#)]
44. Xiao, R.; Wang, Q.; Zhang, M.; Pan, W.; Wang, J.J. Plankton distribution patterns and the relationship with environmental gradients and hydrological connectivity of wetlands in the Yellow River Delta. *Ecohydrol. Hydrobiol.* **2020**, *20*, 584–596. [[CrossRef](#)]
45. Vogt, P.; Ferrari, J.R.; Lookingbill, T.R.; Gardner, R.H.; Riitters, K.H.; Ostapowicz, K. Mapping functional connectivity. *Ecol. Indic.* **2009**, *9*, 64–71. [[CrossRef](#)]
46. Soille, P.; Vogt, P. Morphological segmentation of binary patterns. *Pattern Recognit. Lett.* **2009**, *30*, 456–459. [[CrossRef](#)]
47. Liu, Y.; Huang, T.-T.; Zheng, X. A method of linking functional and structural connectivity analysis in urban green infrastructure network construction. *Urban Ecosyst.* **2022**, 1–17. [[CrossRef](#)]
48. Dai, J.; Liu, X.; Hu, F. Research and Application for Grey Relational Analysis in Multigranularity Based on Normality Grey Number. *Sci. World J.* **2014**, *2014*, 1–10. [[CrossRef](#)]
49. Huimin, L. The impact of human behavior on ecological threshold: Positive or negative?—Grey relational analysis of ecological footprint, energy consumption and environmental protection. *Energy Policy* **2013**, *56*, 711–719. [[CrossRef](#)]
50. Xu, M.; Zhu, Q.; Wu, J.; He, Y.; Yang, G.; Zhang, X.; Li, L.; Yu, X.; Peng, H.; Wang, L. Grey relational analysis for evaluating the effects of different rates of wine lees-derived biochar application on a plant–soil system with multi-metal contamination. *Environ. Sci. Pollut. Res.* **2017**, *25*, 6990–7001. [[CrossRef](#)]
51. Kuo, Y.; Yang, T.; Huang, G.-W. The use of grey relational analysis in solving multiple attribute decision-making problems. *Comput. Ind. Eng.* **2008**, *55*, 80–93. [[CrossRef](#)]
52. Mann, H.B. Nonparametric tests against trend. *Econometrica* **1945**, *13*, 245–259. [[CrossRef](#)]
53. Du, J.; Wang, K.; Cui, B.; Jiang, S. Correction of Inhomogeneities in Observed Land Surface Temperatures over China. *J. Clim.* **2020**, *33*, 8885–8902. [[CrossRef](#)]
54. Cao, R.; Jia, X.; Huang, L.; Zhu, Y.; Wu, L.; Shao, M. Deep soil water storage varies with vegetation type and rainfall amount in the Loess Plateau of China. *Sci. Rep.* **2018**, *8*, 12346. [[CrossRef](#)] [[PubMed](#)]
55. Sun, G.; Zhou, G.; Zhang, Z.; Wei, X.; McNulty, S.; Vose, J.M. Potential water yield reduction due to forestation across China. *J. Hydrol.* **2006**, *328*, 548–558. [[CrossRef](#)]
56. Yu, Z.; Liu, S.; Wang, J.; Wei, X.; Schuler, J.; Sun, P.; Harper, R.; Zegre, N. Natural forests exhibit higher carbon sequestration and lower water consumption than planted forests in China. *Glob. Chang. Biol.* **2018**, *25*, 68–77. [[CrossRef](#)]
57. Fierro, A.; Grez, A.A.; Vergara, P.M.; Ramírez-Hernández, A.; Micó, E. How does the replacement of native forest by exotic forest plantations affect the diversity, abundance and trophic structure of saproxylic beetle assemblages? *For. Ecol. Manag.* **2017**, *405*, 246–256. [[CrossRef](#)]
58. Valipour, M. Importance of solar radiation, temperature, relative humidity, and wind speed for calculation of reference evapotranspiration. *Arch. Agron. Soil Sci.* **2014**, *61*, 239–255. [[CrossRef](#)]
59. Liu, X.; Zhang, D. Trend analysis of reference evapotranspiration in Northwest China: The roles of changing wind speed and surface air temperature. *Hydrol. Process.* **2013**, *27*, 3941–3948. [[CrossRef](#)]